



The impact of monoaromatic hydrocarbons on OH reactivity in the coastal UK boundary layer and free troposphere

R. T. Lidster¹, J. F. Hamilton¹, J. D. Lee^{1,2}, A. C. Lewis^{1,2}, J. R. Hopkins^{1,2}, S. Punjabi¹, A. R. Rickard^{1,2}, and J. C. Young³

¹The Department of Chemistry, The University of York, Heslington, UK

²National Centre for Atmospheric Science, University of York, Heslington, York, UK

³School of Chemistry, University of Leeds, Leeds, UK

Correspondence to: J. F. Hamilton (jacqui.hamilton@york.ac.uk)

Received: 31 October 2013 – Published in Atmos. Chem. Phys. Discuss.: 10 December 2013

Revised: 22 April 2014 – Accepted: 9 May 2014 – Published: 2 July 2014

Abstract. Reaction with the hydroxyl radical (OH) is the dominant removal mechanism for virtually all volatile organic compounds (VOCs) in the atmosphere; however, it can be difficult to reconcile measured OH reactivity with known sinks. Unresolved higher molecular weight VOCs contribute to OH sinks, of which monoaromatics are potentially an important sub-class. A method based on comprehensive two-dimensional gas chromatography coupled to time-of-flight mass spectrometry (GC × GC-TOFMS) has been developed that extends the degree with which larger VOCs can be individually speciated from whole air samples (WAS). The technique showed excellent sensitivity, resolution and good agreement with an established gas chromatography–flame ionisation (GC-FID) method, for compounds amenable to analysis on both instruments. Measurements have been made of VOCs within the UK east coast marine boundary layer and free troposphere, using samples collected from five aircraft flights in winter 2011. Ten monoaromatic compounds with an array of different alkyl ring substituents have been quantified, in addition to the simple aromatics, benzene, toluene, ethyl benzene and Σ *m*- and *p*-xylene. These additional compounds were then included in constrained box model simulations of atmospheric chemistry occurring at two UK rural and suburban field sites in order to assess the potential impact of these larger monoaromatic species on OH reactivity; they have been calculated to contribute an additional 2–6% to the overall modelled OH loss rate, providing a maximum additional OH sink of $\sim 0.9\text{ s}^{-1}$.

1 Introduction

It is well known that the hydroxyl radical (OH) controls the daylight oxidising capacity of the atmosphere (Heard and Pilling, 2003). In the presence of NO_x and volatile organic compounds (VOCs), reactions involving OH can contribute to the formation of a range of important secondary pollutants, including tropospheric ozone, NO₂ and secondary organic aerosol (SOA) (Atkinson, 2000; Goldstein and Galbally, 2007). The OH concentration, [OH], is controlled partly by species emitted from biogenic and anthropogenic sources acting as both precursors and reactive sinks. Due to the high reactivity of OH ($\tau_{\text{OH}} = 0.01\text{--}1.00\text{ s}$), the effects of air mass transport can be ignored and its concentration is dependant only on the in situ chemical environment and solar irradiance (Logan et al., 1981). In recent years, the in situ measurement of OH reactivity has become a useful tool for assessing our understanding of the reactive sinks for OH in different environments (Kovacs and Brune, 2001; Di Carlo et al., 2004; Sadanaga et al., 2004; Sinha et al., 2008; Nölscher et al., 2012). This is typically performed either via a “pump and probe” (Sadanaga et al., 2004), discharge flow techniques (Kovacs and Brune, 2001; Di Carlo et al., 2004) or a comparative reactivity method (Sinha et al., 2008; Nölscher et al., 2012). The former uses a laser pulse to generate OH radicals within a reaction cell and, using laser-induced fluorescence (LIF), detect the OH concentration decay with time as ambient air is introduced. The discharge flow method differs in the OH generation mechanism. Here OH radicals are generated using a mercury UV lamp and injected into a large

flow tube with ambient air. The subsequent OH decay is then monitored by LIF. The comparative reactivity method uses a competitive reaction of artificially produced OH radicals with a reagent not typically present in air (e.g. pyrrole) (Sinha et al., 2008; Nölscher et al., 2012). The reagent is monitored at three stages: (1) before reaction with OH, (2) after OH processing and (3) after OH processing in the presence of ambient air. The difference in concentration of the reagent in the presence of, and absence of, ambient air can be attributed to the OH reactivity of that sample.

A total OH reactivity measurement has the advantage of replacing many individual species measurements and includes species which are either not currently measured or are not known. By making comparisons of OH reactivity data with model predictions, our current understanding of tropospheric oxidation mechanisms can be tested. Previous reactivity studies have shown that OH loss processes are not always fully accounted for, with the *in situ* measurement of OH reactivity being higher than the sum of all measured individual sinks. Several studies propose that unmeasured species are responsible for the discrepancy. VOCs provide a major loss route for the OH radical in the atmosphere, and it has been suggested that unmeasured VOC species may account for the discrepancy in OH reactivity (Di Carlo et al., 2004; Mao et al., 2009; Lee et al., 2009). Complete characterisation of all these loss pathways, however, is a major analytical challenge due to the degree of isomeric and functional complexity present in atmospheric air samples (Lewis et al., 2000; Goldstein and Galbally, 2007).

Hyphenated chromatographic techniques have become increasingly popular as a way to improve the identification and quantification of VOCs in the atmosphere. Comprehensive two-dimensional gas chromatography (GC × GC) involves the coupling of two columns with different separation mechanisms via a mid-point modulator. The technique was first performed by Phillips and Liu (1991) on petrochemical mixtures and has since enabled the separation of high-complexity samples in a range of fields, giving separations that were previously unattainable by conventional capillary GC and GC-MS methods.

The first GC × GC analysis of VOCs in air was performed by Lewis et al. (2000) with a flame ionisation detector (FID). This identified that much of the hydrocarbon loading in an urban atmosphere was unaccounted for using conventional one-dimensional GC-FID techniques. Hamilton and Lewis (2003) reported the monoaromatic composition of gasoline, gasoline vapours and urban air samples using GC × GC-FID with a simple cooled loop injection. They found that many of the larger aromatic species present in gasoline vapour were also present in urban air. A total of 147 monoaromatic isomers were isolated from a polluted urban air sample and were calculated to be a potentially significant source of tropospheric ozone. GC × GC has subsequently been used in a range of studies of atmospheric composition at locations with

different sources and degrees of ageing (Xu et al., 2003a, b; Lee et al., 2006; Bartenbach et al., 2007; Saxton et al., 2007).

The complex nature of the chromatograms and the huge quantity of data produced has led to very few quantitative studies of the atmosphere using GC × GC, although, coupled to more traditional quantitative techniques, it has the potential to lead to improvements in our understanding of the organic complexity of the atmosphere.

This paper presents the development of a quantitative method for the analysis of atmospheric VOCs using GC × GC-TOFMS (gas chromatography coupled to time-of-flight mass spectrometry), tailored to clean boundary layer and free-tropospheric samples. The method was used for off-line analysis of whole air samples (WAS) taken onboard the UK Facility for Airborne Atmospheric Measurement's (FAAM) BAe-146 atmospheric research aircraft (ARA) during the winter 2011 Role of Nighttime chemistry in controlling the Oxidising Capacity of the atmosphere (RONOCO) flying campaign.

The linearity and precision of the method were investigated and the measurement compared to a well-established GC-FID system. The impact of a small subset of monoaromatic species that are rarely reported in routine analysis has been investigated on OH reactivity using a constrained box model incorporating the Master Chemical Mechanism (MCMv3.1, <http://mcm.leeds.ac.uk/MCM>) to simulate summertime photochemistry occurring at two UK field sites: (1) on the rural edge of London and (2) on the north Norfolk coast.

2 Experimental

2.1 The RONOCO campaign

The RONOCO project (RONOCO, 2009–2011) involved an aircraft campaign to obtain comprehensive measurements of nighttime atmospheric composition in order to further our understanding of chemistry occurring at night. The campaign was conducted using FAAM BAe-146 aircraft in two campaigns: July 2010 (summer) and January 2011 (winter). Flights were performed from East Midlands Airport, with most of the sampling occurring off the east or south coast of the UK (WAS sampling locations and flight tracks are shown in Fig. 1). The FAAM large Atmospheric Research Aircraft (ARA) is a modified BAe-146 airliner (BAe-146-301) with a range of approximately 1800 nautical miles (3340 km), a ceiling altitude of 35 000 ft (10.7 km) and a maximum flight duration 5 h, carrying 3 crew and up to 18 scientists. During the RONOCO campaign, measurements were made of a number of trace gases including carbon monoxide (CO), ozone (O₃), oxides of nitrogen (NO and NO₂), non-methane hydrocarbons (NMHC), oxygenated volatile organic compounds (OVOC), dinitrogen pentoxide (N₂O₅) and radical intermediates (NO₃, OH and HO₂). In addition, aircraft

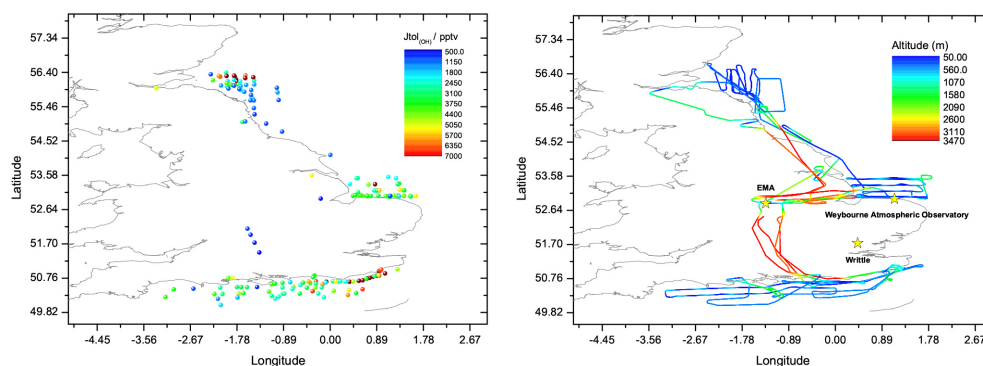


Figure 1. WAS locations analysed using GC × GC-TOF-MS during the RONOCO campaign. Left: spatial distribution of WAS bottles, coloured by their respective total $[EQ_{\text{Tol}}]_{\text{OH}}$ value. Right: flight Tracks for the five RONOCO flights in which GC × GC-TOFMS analysis was performed, coloured by altitude. EMA = East Midlands Airport.

positional data were recorded, along with temperature, pressure, humidity and turbulence.

The FAAM ARA has the facility to accommodate a total of 64 WAS canisters used for collection of air samples during flight. The stainless steel canisters are 3 L in volume and the interior has been coated with a layer of deactivated silica (Silcosteel). The canisters, once fitted into the hold of the aircraft, are filled at various points during flights using an all stainless steel assembly and double-headed metal bellows pump. Canisters are typically filled to their maximum fill pressure of 3 atm, giving a sample volume of approximately 9 L. The fill pressure is reduced at higher altitudes, but typically always remains above 2 atm. The filling duration and frequency of the sampling is user-controlled; filling times are increased at higher altitudes to ensure adequate fill pressure but range from 30 to 120 s for altitudes of 50–7000 m. The individual WAS canisters are housed in metal flight cases of between 8 and 15 bottles. Within these cases, bottles are connected together via a common inlet and outlet port. Individual canisters are filled via electronic activation of pneumatic solenoid valves that are controlled by a personal computer (PC) within the aircraft cabin. WAS canisters can be filled at a desired point in the flight or set to automatically fill at regular time intervals using the WAS filling software. All fittings, connectors and gauges used on the WAS case and aircraft assembly are 316 stainless steel to eliminate contamination; this type of stainless steel has been shown to provide minimal losses for NMHCs also measured in situ (Stone et al., 2010). The analysis of the WAS canisters was performed within three days of sample collection; the stability of a range of compounds of functionalities and volatilities similar to those in this study were investigated and found to be acceptable within the analysis time frame (see supplementary data).

2.2 Gas sampling

A schematic of the instrument setup is shown in Fig. 2. Gas sampling and thermal desorption (TD) was performed using a Markes Unity 2 with CIA8 (Markes International, Llantrisant, UK) using a general purpose hydrocarbon sorbent trap (Markes International). For WAS samples, the Unity 2 used the following settings. The sorbent trap was cooled to 10 °C and trapping was performed at 100 mL min⁻¹ for 10 min, giving a 1 L sample volume. The trap was then purged for a further 10 min with helium carrier gas, while maintaining 10 °C, to ensure the majority of trapped water was removed. For injection onto the GC × GC system, the trap was rapidly heated to 250 °C at > 100 °C s⁻¹. The transfer line was heated to 200 °C and all other flow paths were heated to 150 °C. A post-sampling line purge was performed for 3 min using carrier gas to ensure the lines were conditioned and cleaned before analysis of the next sample. To prevent excessive trapping of water, a 200 mL cold finger submerged in an ethylene glycol water chiller set at -30 °C was used during all of the atmospheric gas analysis. Cold fingers have been used extensively in previous atmospheric studies and have shown to be a suitable water removal method for the analysis of a range of compounds of different functionalities and vapour pressures (Hopkins et al., 2006, 2011; Apel et al., 2008; Lewis et al., 2013). Tests were also performed as part of this study, and they found there to be no issue in the use of a cold finger for the compounds discussed in this investigation (see the Supplement). To ensure each sample was effectively flushed through the cold finger before sampling onto the sorbent trap, a pre-sampling line purge was performed for 5 min at 100 mL min⁻¹. The analysis of the WAS canisters was performed within three days of sample collection, the stability of a range of compounds of functionalities and volatilities similar to those in this study were investigated and found to be acceptable within the analysis time frame (see supplementary data).

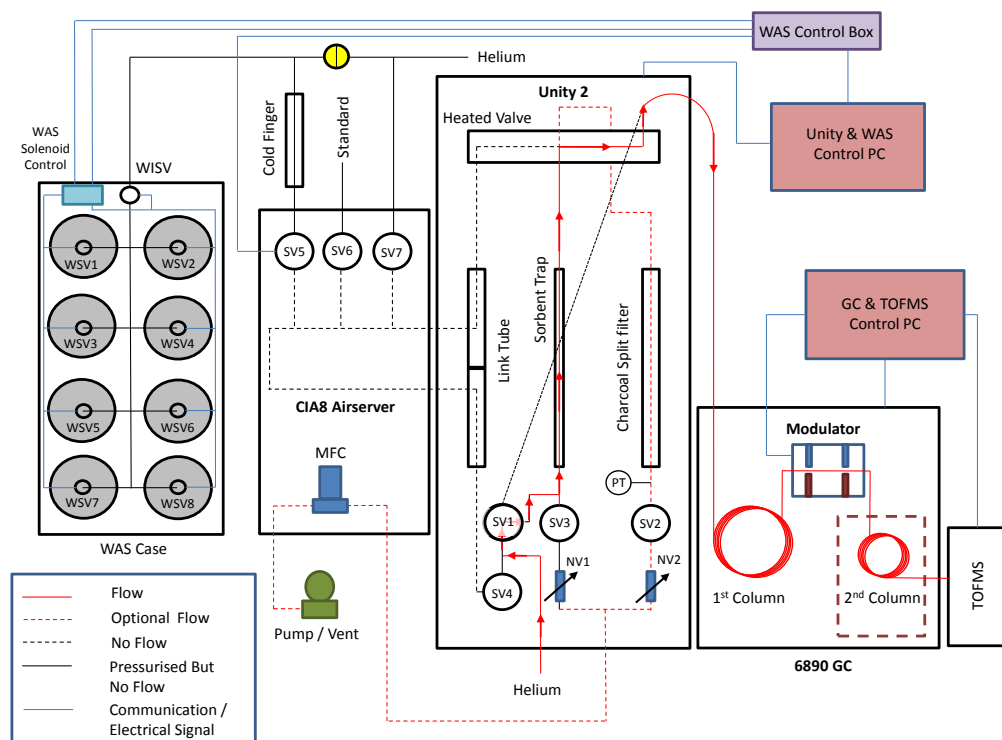


Figure 2. Schematic of the finalised TD-GC × GC-TOFMS sampling setup. SV stands for solenoid valve, NV for needle valve, MFC for mass flow controller, WISV for WAS inlet solenoid valve, WSV for WAS solenoid valve, and PT for pressure transducer.

Activation of the correct WAS bottle was achieved using an in-house control box, programmed via LabVIEW, which activated the electronic solenoid valve of the desired WAS bottle. A contact closure was sent using a relay connected to the sampling port valve on the CIA8. During the Unity's pre-purge step the air server sample valve was opened, triggering the opening of the desired canister. The length of time the WAS canister remained open was also controlled by software. The software was set to leave the WAS bottle open slightly longer than the Unity in order to ensure the software did not trigger the opening of another WAS bottle prematurely. Connections between the CIA8, the cold finger and the WAS bottles were made using 1.6 mm (OD) instrument-grade stainless steel (Thames Restek UK Ltd), which were heated and insulated to approximately 70 °C. Narrow-bore tubing was used to reduce dead volume, ensuring the line was thoroughly flushed during the pre-purge step of the next sample.

2.3 TD-GC × GC-TOFMS

The TD-GC × GC-TOFMS consisted of an Agilent 6890 (Agilent Technologies, Palo Alto, CA, USA) gas chromatograph and a Pegasus III TOF-MS (Leco, St. Joseph, MI, USA). Integration and data processing were performed using ChromaTOF 3.32 software (Leco, St. Joseph, MI, USA) optimised for Pegasus data files. The primary column was

a non-polar BPX-5 (50 m × 0.32 mm 1.0 µm column film thickness) (SGE Analytical Science) and the secondary column a Rtx50 (4.5 m × 0.18 mm × 0.2 µm *d.f.* film thickness) (Thames Restek UK Ltd). The two columns were coupled by means of a glass press fit connector and the secondary column was housed in a secondary oven in the main GC oven. Helium carrier gas was used in constant pressure mode set at 275 kPa (chemically pure grade, BOC) and was set using the Unity 2. The GC oven was configured with the following parameters. An initial temperature of 40 °C held for 4 min, then the oven was ramped at 3 °C min⁻¹ to 160 °C, further ramped at 50 °C min⁻¹ to 200 °C and held for 1.2 min. The secondary oven used the same parameters; however, it was offset by +25 °C. The modulator temperature offset was set at +45 °C and a modulation time of 2 s was used. The TOFMS was set to an acquisition rate of 100 Hz using a detector voltage of 1950 V and a filament bias of -70 eV and acquired for a mass range of *m/z* 35 to 300. The ion source and transfer line were both set to 250 °C and a 2 min solvent delay was used. Peak quantification was performed using the summed peak area from each modulation pulse (3-D volume). The whole system has a sample turnaround time of just under 1 h and has precision and limits of detection ranging from 0.6 to 15 % and 0.01 to 0.2 pptv for a range of NMHCs detailed in Table 1.

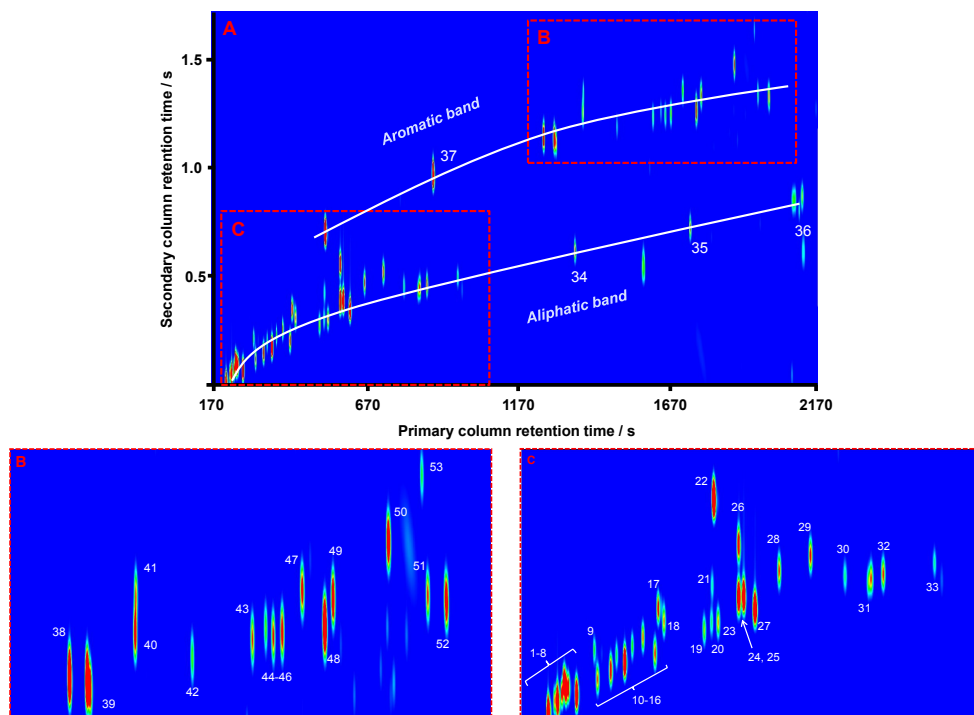


Figure 3. (A) TD-GC × GC-TOFMS chromatogram of the AR74 HC standard. Labelled peaks are identified as follows: (34) nonane; (35) decane; (36) undecane and (37) toluene. (B) shows the aromatic region of the chromatogram. Labelled peaks are identified as follows: (38) ethyl benzene; (39) *m/p*-xylene, (40) *o*-xylene, (41) styrene, (42) isopropyl benzene, (43) propyl benzene, (44) 3-ethyltoluene, (45) 4-ethyltoluene, (46) 1,3,5-trimethylbenzene, (47) 2-ethyl toluene, (48) *t*-butylbenzene, (49) 1,2,4-trimethylbenzene, (50) 1,2,3-trimethylbenzene, (51) 1,3-diethylbenzene, (52) 1,4-diethylbenzene and (53) indane. (C) shows the aliphatic region. Labelled peaks are identified as follows: (1) 2-methylbutane, (2) pentane, (3) 1-pentene, (4) E-2-pentene, (5) isoprene, (6) Z-2-pentene, (7) 2-methyl-2-butene, (8) 2,2-dimethylbutane, (9) cyclopentene, (10) 2-methylpentane, (11) 3-methylpentane, (12) 2-methyl-1-pentene, (13) hexane, (14) E-2-hexene, (15) Z-2-hexene, (16) 2,4-dimethylpentane, (17) 1,3-hexadiene, (18) methylcyclopentane, (19) 2-methylhexane, (20) 2,3-dimethylpentane, (21) cyclohexane, (22) benzene, (23) 3-methylhexane, (24) 1,3-dimethylcyclopentane, (25) 1-heptene, (26) cyclohexene, (27) heptane, (28) 2,3-dimethyl-2-pentene, (29) methylcyclohexane, (30) 2,3,4-trimethylpentane, (31) 2/4-methylheptane, (32) 3-methylheptane and (33) octane.

2.4 Calibration

Method development, calibrations and quantification were performed using a series of parts per billion by volume (ppbv) gas standards; NPL30 ozone precursor mix and terpene standard (National Physical Laboratory, Teddington, UK), and AR54 and AR74 hydrocarbon standards (Apel-Reimer, Boulder, CO, USA). Various volumes and replicates were sampled for method validation. Calibration of the TD-GC × GC-TOFMS system during the RONOCO flying campaign was performed using a combination of the AR54 and the AR74 gas standards. The standards were run as frequently as possible to ensure accurate quantification and to minimise uncertainty due to MS detector drift. The AR54 hydrocarbon standard was analysed every time new WAS cases were connected to the instrument (every 8 to 16 samples). The AR74 hydrocarbon standard was run less frequently, once every 24 h or every 24 samples depending on which occurred first, due to limited standard availability.

2.5 FGAM DC-GC-FID

The samples were also analysed using a single-column, dual-channel FID system (DC-GC-FID), which is well established and operated by the NCAS Facility for Ground Atmospheric Measurements (FGAM). The system uses two GC columns running in parallel. After sampling and desorption, the flow is split 50 : 50 and passes down a aluminium oxide (Al₂O₃) porous layer open tubular (PLOT) column (50 m, 0.53 mm ID) for analysis of NMHCs and two LOWOX columns (10 m, 0.53 mm ID) in series for analysis of OVOCs. The instrument setup and operation is described in detail in Hopkins et al. (2006, 2011). Calibrations were performed using a 30-component ppbv-level ozone precursor standard, NPL30 (National Physics Laboratory). The FGAM DC-GC-FID system has a sample turnaround time of 1 h and has limits of detection in the range of 0.5–6 pptv for NMHCs (Hopkins et al., 2006).

3 Results and discussion

The TD-GC × GC-TOFMS system was calibrated using a series of gas standards and an example chromatogram is shown in Fig. 3, where the retention times in columns 1 and 2 are shown on the x and y axes respectively and the peak intensity shown as a coloured contour. The instrument shows excellent separation of the hydrocarbons with $>C_5$, with the exception of *m/p*-xylene as seen in most GC separations using siloxane columns. No signals were seen for hydrocarbons with less than five carbons as they were too volatile to be retained on the liquid nitrogen modulator. An advantage of GC × GC is that compounds elute in characteristic patterns depending on their functionality. This pattern can be observed in Fig. 3, with the aromatic species well separated from the aliphatics in the second dimension. Precision, limits of detection (LOD) and linearity of calibration for the species calibrated using gas standards are shown in Table 1. The relative standard deviation was calculated for five replicate injections of a 1 L sample of the AR74 hydrocarbon standard at ~ 100 pptv, and the R^2 value given is for a six-point calibration ranging from approximately 10 to 250 pptv (depending on the standard mixing ratio of each compound). The limit of detection was calculated at $S/N = 3$. The retention time and quantification ion used for the calibration are also shown.

The TD-GC × GC-TOFMS was able to consistently resolve the majority of species in the gas standard with relative standard deviation (%RSD) values less than 5%, with the exception of 1-pentene, *cis*-2-pentene and 2-methyl-2-butene that gave a higher %RSD. These compounds co-elute with each other on the column set used and have similar mass spectra leading to poor mass spectral deconvolution. Limits of detection for a 1 L sample were found to be generally sub-pptv and calibrations showed good linearity ($R^2 > 0.99$). These results show that the GC × GC-TOFMS is both highly sensitive and a high-resolution analysis technique. The low detection limits observed are a result of peak amplitude enhancement from the thermal modulator; the improved background inherent to GC × GC when multiple isomers are present; and the TOFMS detector, which allows characteristic ions to be extracted from the complex air background, removing background interferences.

3.1 Inter-comparison with FGAM DC-GC-FID

During the RONOCO campaign, the WAS were analysed by both TD-GC × GC-TOFMS and TD-GC-FID. The dual-channel GC-FID method is well established and is tailored for the analysis of NMHCs from C_2 to C_8 , with limits of detection typically between 1 and 5 pptv. Due to the selectivity required for the analysis of very volatile hydrocarbons, the GC-FID system's performance is reduced as the molecular weight of hydrocarbons increases. This results in broadening of the chromatographic peaks and reduced signal to noise for these species. It is important to consider that as carbon num-

ber increases, the potential number of isomers for hydrocarbon species increases exponentially, and so the potential for co-elution of species within this heavier region of a GC run becomes more likely with single-column techniques (Goldstein and Galbally, 2007).

The mixing ratios obtained by both techniques for 191 WAS bottles collected during RONOCO were plotted against each other in order to compare the performance achieved for actual air samples. In total seven compounds (pentane, hexane, heptane, octane, benzene, toluene and ethylbenzene) were common between both analyses. Good correlations were observed ($R^2 = 0.93$ – 0.99) for all species. The higher molecular weight alkanes, heptane and octane, showed a good correlation between the two techniques, as shown in Fig. 4; however, there is a deviation from the 1 : 1 line. These large VOCs are at the volatility and separation limit of the GC-FID system. For heptane and octane, it should also be noted that the levels detected are typically lower than many other hydrocarbon species detected. There are many samples where the octane and heptane levels fall below the limit of detection for the GC-FID instrument and appear as a space in the GC-FID bottle series shown in the left-hand panels of Fig. 4. However, for these samples, the GC × GC-TOFMS was able to quantify the species due to its better LOD.

The increased sensitivity of the GC × GC-TOFMS system is once again noticeable for the comparison with octane, where some of the samples are below the LOD of the GC-FID method but are successfully quantified by GC × GC-TOFMS. Very good agreement was seen for the aromatic species, toluene and benzene, between the two techniques, as shown in Fig. 3, with both high R^2 values and slopes very close to 1 : 1. Good correlations of the aromatic species are particularly useful as they validate that the GC × GC-TOFMS is functioning correctly with no leaks.

3.2 Analysis of VOCs using GC × GC-TOFMS during the RONOCO campaign

In total, 191 WAS bottles from five flights were analysed by TD-GC × GC-TOFMS over a 3-week period. Samples were collected between 60 and 3500 m altitude, generally over the North Sea or English Channel. A typical GC × GC chromatogram can be observed in Fig. 5 for a WAS canister taken in the English Channel at $50^{\circ}20'45.15''$ N, $1^{\circ}39'25.42''$ W on the 21 January 2011 at 16:45 UTC. The structure of the GC × GC chromatogram is visible, with the unsaturated aliphatics and aromatics well resolved from the aliphatic band. The complexity of the sample is apparent and is further complicated by the presence of many oxygenated and other functionalised species, which co-elute with the aromatic band. The TOFMS is particularly useful for the identification of analytes against the NIST Mass Spectral library and also allows for simplification of the chromatogram as ions characteristic to particular functional groups can be

Table 1. List of quantifiable compounds and validation parameters for the AR74 hydrocarbon standard using GC×GC-TOFMS. Grouped by functionality and compounds given in retention order.

Compound	RT (1D/s, 2D/s ^a)	Quant Mass ^b	%RSD ^c	LOD/pptv ^d	R ² ^e	Fig. ref ^f
Alkanes						
Butane, 2-methyl-	222, 0.020	57.00	0.63	0.16	0.9917	3 – 1
Pentane	242, 0.060	57.00	4.96	0.13	0.9920	3 – 2
Butane, 2,2-dimethyl-	278, 0.070	57.00	0.79	0.04	0.9992	3 – 8
Cyclopentane	328, 0.210	70.00	5.07	0.61	0.9967	–
Pentane, 2-methyl-	320, 0.130	71.00	0.56	0.03	0.9990	3 – 10
Pentane, 3-methyl-	346, 0.160	57.00	1.00	0.04	0.9999	3 – 11
Hexane	374, 0.180	57.00	1.51	0.05	0.9978	3 – 13
Pentane, 2,4-dimethyl-	432, 0.210	57.00	0.63	0.04	0.9997	3 – 16
Cyclopentane, methyl-	450, 0.310	56.00	0.89	0.04	0.9990	3 – 18
Hexane, 2-methyl-	528, 0.280	57.00	1.14	0.06	0.9995	3 – 19
Pentane, 2,3-dimethyl-	542, 0.300	57.00	1.46	0.08	0.9984	3 – 20
Cyclohexane	544, 0.430	84.00	3.74	0.28	0.9985	3 – 21
Hexane, 3-methyl-	556, 0.310	57.00	1.37	0.06	0.9992	3 – 23
Pentane, 2,2,4-trimethyl-	590, 0.290	57.00	3.53	0.05	0.9993	–
Cyclopentane, 1,3-dimethyl-	596, 0.390	70.00	1.73	0.06	0.9981	3 – 24
Heptane	628, 0.350	71.00	1.75	0.08	0.9977	3 – 27
Cyclohexane, methyl-	736, 0.520	83.00	1.08	0.03	0.9984	3 – 29
Pentane, 2,3,4-trimethyl-	804, 0.450	71.00	1.51	0.04	0.9991	3 – 30
Heptane, 2/4-methyl-	850, 0.430	70.00	2.15	0.07	0.9992	3 – 31
Heptane, 3-methyl-	880, 0.460	57.00	2.50	0.05	0.9985	3 – 32
Octane	980, 0.490	57.00	7.17	0.09	0.9991	3 – 33
Nonane	1362, 0.610	57.00	3.78	0.05	0.9996	3 – 34
Decane	1738, 0.700	57.00	4.53	0.05	0.9988	3 – 35
Undecane	2094, 0.780	57.00	5.16	0.08	0.9984	3 – 36
Alkenes						
1-Pentene	236, 0.060	55.00	9.70	0.07	0.9930	3 – 3
2-Pentene, (E)-	250, 0.080	55.00	2.41	0.03	0.9998	3 – 4
2-Pentene, (Z)-	258, 0.100	55.00	14.78	0.01	0.9992	3 – 6
2-Butene, 2-methyl-	262, 0.100	55.00	7.31	0.03	0.9932	3 – 7
Cyclopentene	314, 0.220	67.00	3.46	0.02	0.9902	3 – 9
1-Pentene, 2-methyl-	358, 0.200	56.00	3.03	0.05	0.9990	3 – 12
2-Hexene, (E)-	388, 0.230	55.00	0.71	0.04	0.9960	3 – 14
2-Hexene, (Z)-	408, 0.260	55.00	1.25	0.05	0.9994	3 – 15
1,3-Hexadiene	438, 0.360	67.00	5.59	0.04	0.9996	3 – 17
Cyclohexene	596, 0.560	67.00	1.24	0.04	0.9991	3 – 26
1-Heptene	606, 0.390	56.00	3.27	0.09	0.9997	3 – 25
2-Pentene, 2,3-dimethyl-	676, 0.480	83.00	2.88	0.05	0.9990	3 – 28
Aromatics						
Benzene	548, 0.700	78.00	3.58	0.01	0.9994	3 – 22
Toluene	900, 0.960	91.00	5.53	0.03	0.9997	3 – 37
Ethyl benzene	1260, 1.130	91.00	3.57	0.03	0.9997	3 – 38
<i>m/p</i> -xylene	1294, 1.130	91.00	3.36	0.05	0.9993	3 – 39
<i>o</i> -xylene	1388, 1.230	91.00	4.05	0.03	0.9982	3 – 40
Styrene	1390, 1.320	104.00	1.16	0.04	0.9965	3 – 41
Benzene, isopropyl-	1500, 1.170	105.00	2.99	0.02	0.9996	3 – 42
Benzene, propyl-	1616, 1.210	91.00	3.22	0.02	0.9999	3 – 43
Toluene, 3-ethyl-	1642, 1.230	105.00	2.76	0.02	0.9995	3 – 44
Toluene, 4-ethyl-	1658, 1.210	105.00	4.76	0.02	0.9994	3 – 45
Benzene, 1,3,5-trimethyl-	1674, 1.220	105.00	3.78	0.02	0.9991	3 – 46
Toluene, 2-ethyl-	1714, 1.320	105.00	5.01	0.02	0.9997	3 – 47
Benzene, <i>t</i> -butyl-	1758, 1.230	91.00	3.75	0.03	0.9986	3 – 48
Benzene, 1,2,4-trimethyl-	1774, 1.300	105.00	4.88	0.02	0.9992	3 – 49
Benzene, 1,2,3-trimethyl-	1882, 1.440	105.00	3.07	0.03	0.9958	3 – 50
Benzene, 1,3-diethyl-	1958, 1.310	105.00	5.18	0.05	0.9993	3 – 51
Benzene, 1,4-diethyl-	1996, 1.290	105.00	3.47	0.06	0.9995	3 – 52
Indane	1948, 1.600	117.00	2.59	0.02	0.9971	3 – 53
Terpenes						
Isoprene	254, 0.120	67.00	1.24	0.07	0.9986	3 – 5
α -Pinene	1528, 0.920	93.00	0.87	0.08	0.9975	–
β -Pinene	1712, 1.090	93.00	3.96	0.11	0.9956	–
3-Carene	1814, 1.110	93.00	3.44	0.11	0.9960	–
Limonene	1892, 1.140	67.00	2.68	0.11	0.9980	–
Eucalyptol	1916, 1.240	81.00	1.88	0.10	0.9939	–

^a Retention time for primary and secondary column.^b *m/z* ion used for quantification^c % RSD is taken from five replicates.^d The limit of detection (LOD) is taken at S/N = 3^e R² value from a six-point calibration with mixing ratios ranging from ~10 to 250 pptv for a 1 L sample^f Refer to Fig. 3 for position in the chromatogram.

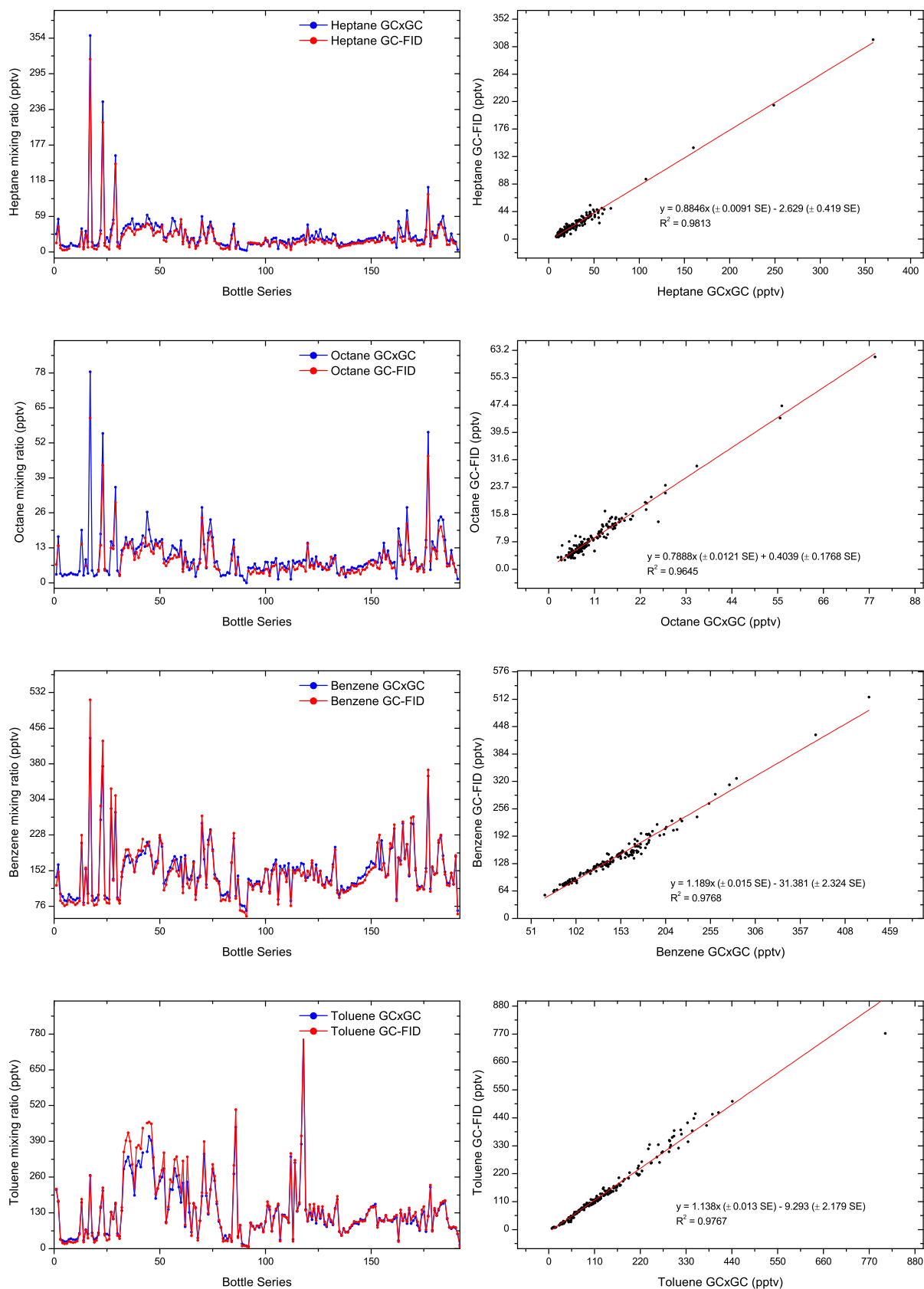


Figure 4. Inter-comparison data for selected compounds measured by both GC × GC-TOFMS and GC-FID.

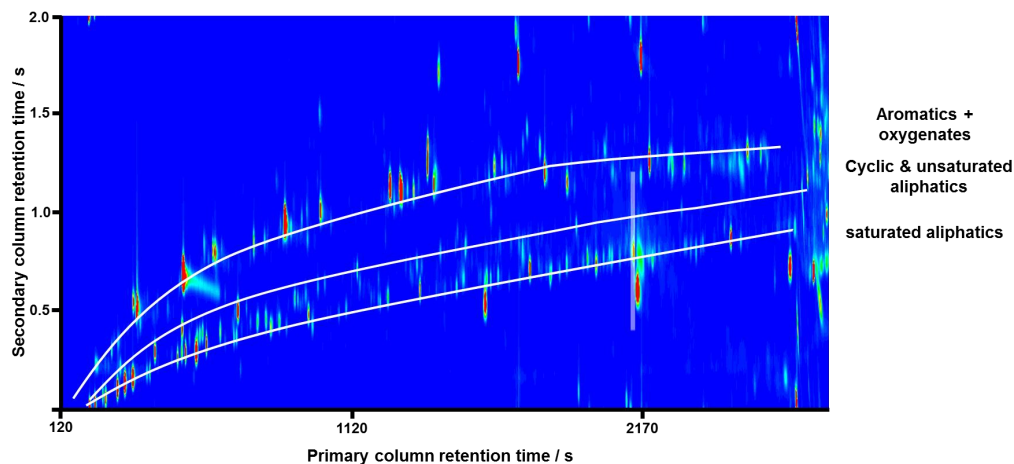


Figure 5. Typical GC × GC-TOFMS chromatogram from RONOCO highlighting the functional group pattern formation.

extracted and viewed in isolation (for example m/z 91 for aromatics).

In total 39 hydrocarbons ranging from C_5 to C_{11} could be quantified during RONOCO using the GC × GC-TOFMS. The mean, minimum and maximum mixing ratios are shown in Table 2 for all samples analysed. The highly substituted aromatic species (C_9 and greater) were observed to exhibit a strong correlation with toluene, as shown in Fig. 6. This can be rationalised due to their similar emission sources (i.e. petrol vapours and evaporation). The alkyl benzenes generally have the same emission sources and so the gradient of the regression line is a result of both emission ratios and reactivity with atmospheric oxidants encountered by the air mass from emission to sampling, assuming the same dilution rate. The higher molecular weight aromatic species may be atmospherically relevant (Hamilton and Lewis, 2003) as many of them exhibit an enhanced reaction rate over toluene with OH and NO_3 radicals (Atkinson and Arey, 2003) and thus they could impact tropospheric ozone formation rates.

The strong linear relationships observed by the GC × GC-TOFMS presents an opportunity to predict the heavier monoaromatic VOC loading by measurement of a toluene mixing ratio alone. This would potentially allow for techniques that cannot analyse these species (GC-FID, PTR-MS etc.) to make a prediction of the additional aromatic content assuming similar emission ratios to those in the UK. For the correlation plots presented in Fig. 6, the intercept in each was set to zero. In order to make a meaningful prediction of the additional aromatic content, a conversion that reflects each aromatic species' concentration and rate of reaction with an atmospheric oxidant is required. This was performed by converting the mixing ratio of each aromatic species into a toluene-equivalent mixing ratio, $[EQ_{Tol}]$. This technique has been used previously in the literature (as a propylene equivalent) to allow atmospheric modellers to simplify VOC data and express them as one variable (Chameides et al., 1992).

The conversion of a mixing ratio into a $[EQ_{Tol}]$ value is performed by multiplying the mixing ratio of the aromatic $[x]$ by the ratio of its rate constant, $k_{OH}(x)$, to that of toluene, $k_{OH}(Toluene)$, as shown in Eq. 1. All aromatic + OH rate coefficients (at 298 K, 1 atm) are taken from Calvert et al. (2002) unless otherwise stated in the text.

$$[EQ_{Tol}] = [x] \frac{k_{OH}(x)}{k_{OH}(Toluene)}. \quad (1)$$

After conversion of the additional aromatic species into a $[EQ_{Tol}]$, the relationship between the toluene mixing ratio and the additional aromatic loading as a $[EQ_{Tol}]$ value was investigated. For all samples analysed using the GC × GC-TOFMS, the mixing ratios of the 10 additional aromatic species (shown in bold in Table 2) were converted to a $[EQ_{Tol}]$ value with respect to both reaction with OH, ($[EQ_{Tol}]_{OH}$) and NO_3 ($[EQ_{Tol}]_{NO_3}$) since many of the samples were taken at night and aromatic reactivity with O_3 is negligible.

As no rate data are currently available in the literature, rate constants for the reactions of 1,3-diethyl benzene and 1,4-diethyl benzene have been calculated using available structure activity relationships (SARs). The SAR approach of Kwok and Atkinson (1995) has been used to estimate total k_{OH} for each diethyl benzene isomer from calculations of partial OH rate constants for hydrogen abstraction from the ethyl groups and OH addition to the aromatic ring. Rate coefficients for OH addition to the ring are estimated from a correlation of the sum of electrophilic substituent constants (Brown and Okamoto, 1958) with measured OH addition rate constants (Calvert et al., 2002). Rate constants for reaction with NO_3 (k_{NO_3}) have been inferred from measured rate data for *m*- and *p*-xylenes (Calvert et al., 2002) using the method applied by Jenkin et al. (2003). As with all estimation methods, there is a reasonable error of uncertainty and as such an error of a factor of 2 should be applied (Kwok and Atkinson, 1995).

Table 2. VOC mixing ratios measured by GC×GC-TOFMS during the winter RONOCO campaign for all samples taken. Bold text shows additional aromatic species featured in this additional reactivity study.

Compound	RT (1-D/s, 2-D/s)	LOD /pptv	Mean /pptv	Median /pptv	MAD ^a /pptv	Min ^b /pptv	Max ^c /pptv
Alkanes							
Pentane	242, 0.060	0.13	133	86	27	10	3213
Butane, 2,2-dimethyl-	278, 0.070	0.04	8.8	7.5	3.4	0.36	55
Pentane, 2-methyl-	320, 0.130	0.03	27	20	8.3	1.3	505
Pentane, 3-methyl-	346, 0.160	0.04	32	25	11	1.8	421
Hexane	374, 0.180	0.05	50	37	13	4.9	838
Pentane, 2,4-dimethyl-	432, 0.210	0.04	4.5	3.7	1.6	0.09	42
Cyclopentane, methyl-	450, 0.310	0.04	30	21	8.9	1.1	515
Hexane, 2-methyl-	528, 0.280	0.06	14	11	4.1	0.95	142
Pentane, 2,3-dimethyl-	542, 0.300	0.08	7.5	5.9	2.5	0.41	78
Cyclohexane	544, 0.430	0.28	19	14	5.2	0.95	286
Hexane, 3-methyl-	556, 0.310	0.06	18	14	5.6	1.2	186
Heptane	628, 0.350	0.08	29	22	8.5	2.4	359
Cyclohexane, methyl-	736, 0.520	0.03	18	12	5.2	0.22	321
Pentane, 2,3,4-trimethyl-	804, 0.450	0.04	4.0	3.7	1.8	0.15	12
Heptane, 2/4-methyl-	850, 0.430	0.07	11	8.9	4.0	0.48	110
Heptane, 3-methyl-	880, 0.460	0.05	4.3	3.6	1.7	0.24	30
Octane	980, 0.490	0.09	9.8	7.6	3.1	1.0	78
Nonane	1362, 0.610	0.05	10	7.8	3.7	0.33	49
Decane	1738, 0.700	0.05	15	12	4.9	0.62	60
Undecane	2094, 0.780	0.08	17	14	4.9	0.12	53
Alkenes							
1-Pentene, 2-methyl-	358, 0.200	0.05	5.6	3.4	1.7	0.40	127
Cyclohexene	596, 0.560	0.04	0.7	0.6	0.29	0.13	3.5
1-Heptene	606, 0.390	0.09	13	8.6	3.4	0.40	261
Styrene	1390, 1.320	0.04	11	15	4.0	0.65	65
Aromatics							
Benzene	548, 0.700	0.01	152	144	28	67	435
Toluene	900, 0.960	0.03	137	107	48	7.8	809
Ethyl benzene	1260, 1.130	0.03	26	21	10	1.2	157
<i>m/p</i> -Xylene	1294, 1.130	0.05	71	59	31	3.6	264
<i>o</i> -Xylene	1388, 1.230	0.03	23	19	9.9	0.91	90
Benzene, isopropyl-	1500, 1.170	0.02	1.5	1.3	0.54	0.08	5.4
Benzene, propyl-	1616, 1.210	0.02	4.7	3.1	1.4	0.09	26
Toluene, 3-ethyl-	1642, 1.230	0.02	11	8.2	4.0	0.31	54
Toluene, 4-ethyl-	1658, 1.210	0.02	5.7	4.2	2.0	0.11	26
Benzene, 1,3,5 trimethyl-	1674, 1.220	0.02	4.7	3.4	1.7	0.11	20
Toluene, 2-ethyl-	1714, 1.320	0.02	5.3	3.9	1.8	0.10	24
Benzene, 1,2,4 trimethyl-	1774, 1.300	0.02	16	12	6.0	1.0	72
Benzene, 1,2,3 trimethyl-	1882, 1.440	0.03	4.2	3.1	1.4	0.38	17
Benzene, 1,3-diethyl-	1958, 1.310	0.05	1.0	0.80	0.50	0.16	3.9
Benzene, 1,4-diethyl-	1996, 1.290	0.06	2.6	2.0	1.0	0.19	9.5

^a The median absolute deviation^b Minimum mixing ratio measured^c Maximum mixing ratio measured

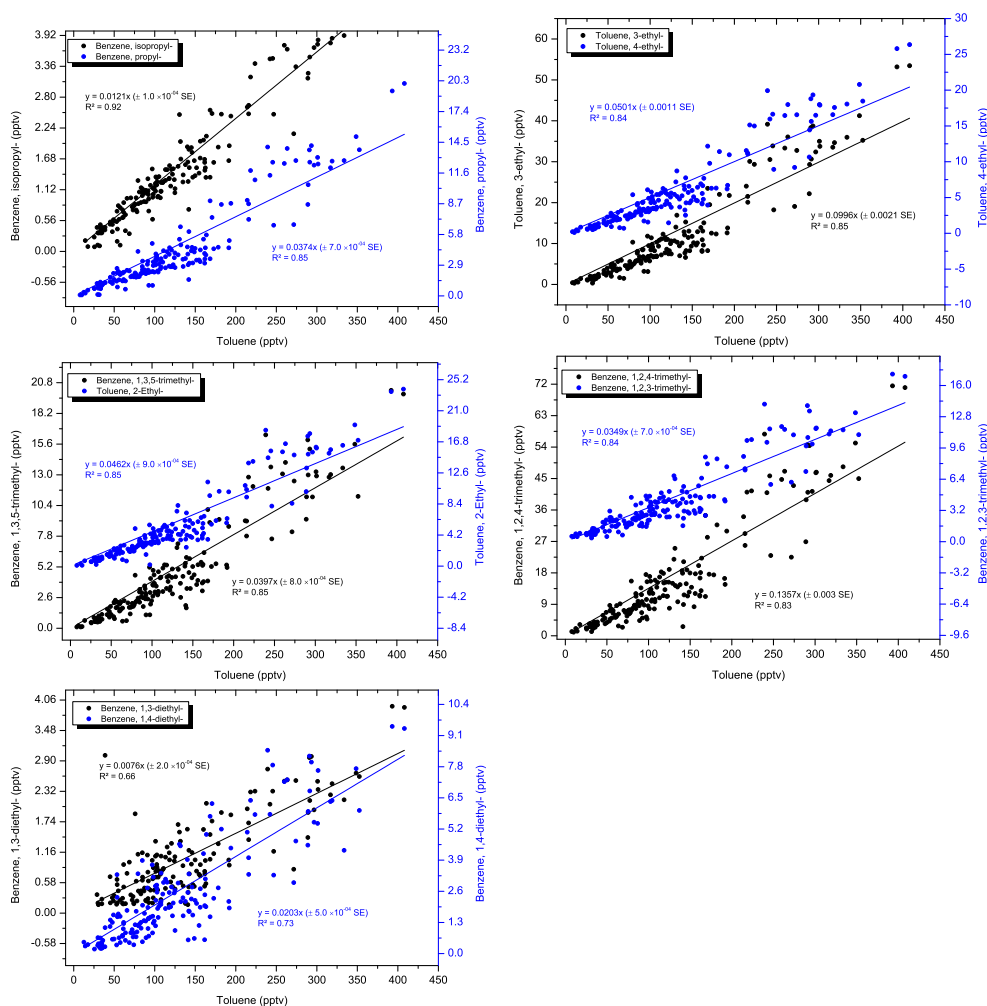


Figure 6. Plots of monoaromatic mixing ratios from each WAS canister against the simultaneous toluene mixing ratio observed. The coefficient of determination and equations of the linear regressions are also given and are also summarised in Table 3.

Table 3. The scaling factors for the 10 additional aromatic species against toluene along with their corresponding R^2 values from the linear regressions in Fig. 6. The 2002 NEI ratio to toluene for comparison.

Species	Slope of regression	R^2	NEI 2002 ratio to toluene
Benzene, isopropyl	0.0121x	0.92	0.0083
Benzene, propyl-	0.0374x	0.85	0.0279
Toluene, 3-ethyl-	0.0996x	0.85	0.0250
Toluene, 4-ethyl-	0.0501x	0.84	0.0102
Benzene, 1,3,5-trimethyl-	0.0397x	0.85	0.1025
Toluene, 2-ethyl-	0.0462x	0.85	0.0002
Benzene, 1,2,4-trimethyl-	0.1357x	0.83	0.2749
Benzene, 1,2,3-trimethyl-	0.0349x	0.84	0.0776
Benzene, 1,3-diethyl-	0.0076x	0.66	0.0067
Benzene, 1,4-diethyl-	0.0203x	0.73	0.0068

The $[EQ_{Tol}]$ values of the 10 individual compounds were then summed for each sample to give a $\Sigma[EQ_{Tol}]$, which represents the additional aromatics measured at each sampling point. The $\Sigma[EQ_{Tol}]$ values were plotted against their respective toluene mixing ratio and are shown in Fig. 7. A reasonable linear relationship is seen with an R^2 of 0.93 and a gradient of 2.03 ± 0.04 and 7.30 ± 0.15 for OH and NO_3 respectively.

The 10 additional monocyclic aromatics may have a considerable effect on reactivity and also potentially ozone formation with a $[EQ_{Tol}]_{OH}$ that is on average twice that of the toluene mixing ratio.

The average contribution of each aromatic species to the $\Sigma[EQ_{Tol}]$ value can be observed in Fig. 8. The tri-substituted benzenes, although at a much lower mixing ratio than toluene (average mixing ratio for 1,3,5 trimethylbenzene is 4.7 ± 0.3 pptv, compared to toluene, which is 136 ± 7 pptv), exhibit a significant rate enhancement for reaction

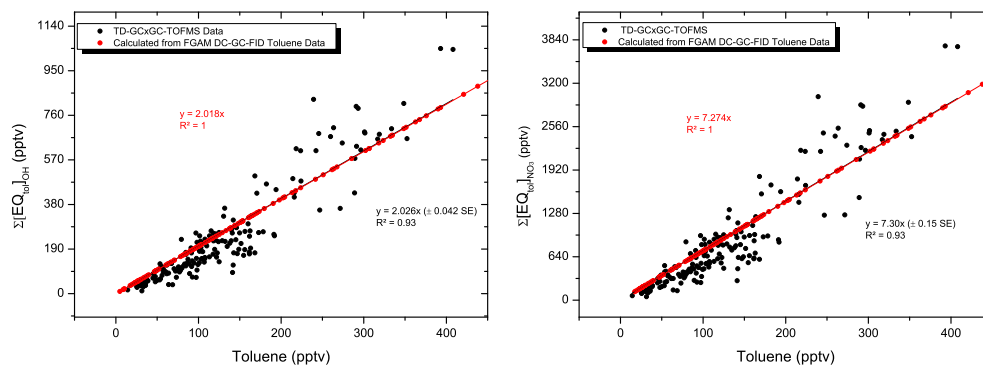


Figure 7. Measured (black) and predicted (red) contribution to $[EQ_{Tol}]$ for aromatic species measured during RONOCO. Left: reactivity with respect to OH ($[EQ_{Tol}]_{OH}$). Right: reactivity with NO_3 ($[EQ_{Tol}]_{NO_3}$). The red trace corresponds to a predicted $\Sigma[EQ_{Tol}]$ value resulting from a measured toluene mixing ratio from the GC-FID system.

with OH (Fig. 8a) and so give rise to large $[EQ_{Tol}]$ values. In contrast to OH, the NO_3 radical exhibits a slower rate of reaction with toluene and other aromatic species. However, the additional aromatic content still adds a large portion of $\Sigma[EQ_{Tol}]_{NO_3}$ when compared to the toluene mixing ratio alone, as shown in Fig. 8b.

A range of different locations off the east and south coast of the UK were sampled during the five RONOCO flights. A summary of the flight tracks and vertical distribution of total $[EQ_{Tol}]_{OH}$ from the aircraft WAS bottles can be observed in Fig. 1. This shows an expected reduction in reactive toluene equivalent with altitude. Variation at lower altitudes is the result of sampling various pollution plumes which result in a sharp rise in hydrocarbon mixing ratios over the background levels.

The FGAM DC-GC-FID used in this study exhibits reduced performance when analysing these aromatic species due to poor peak shape and increased co-elution, which contribute to a higher limit of detection. Using the gradients of linear regressions from the measured GC × GC-TOFMS data and the toluene mixing ratio from the FGAM DC-GC-FID, a prediction of the $\Sigma[EQ_{Tol}]$ value was carried out. The predicted additional aromatic $\Sigma[EQ_{Tol}]$ calculated using the FGAM DC-GC-FID toluene mixing ratio is shown by the red line in Fig. 7. The additional aromatic content calculated using the proportionality factors shows a good level of agreement with the measured values, with a discrepancy between the two trend lines of approximately $< 0.4\%$ for both radical oxidants. The correlation data for each additional aromatic species can be found in Table 3 along with their corresponding R^2 value for the linear regression. The 2002 UK National Emission Inventory (NEI) ratios to toluene are also presented for comparison.

The short daytime lifetimes of these larger molecular weight monoaromatics means the observed daytime ratio to toluene is likely to change depending on the sample's distance from source. The RONOCO flights address this issue as they took place at night (or dawn), resulting in the air mass

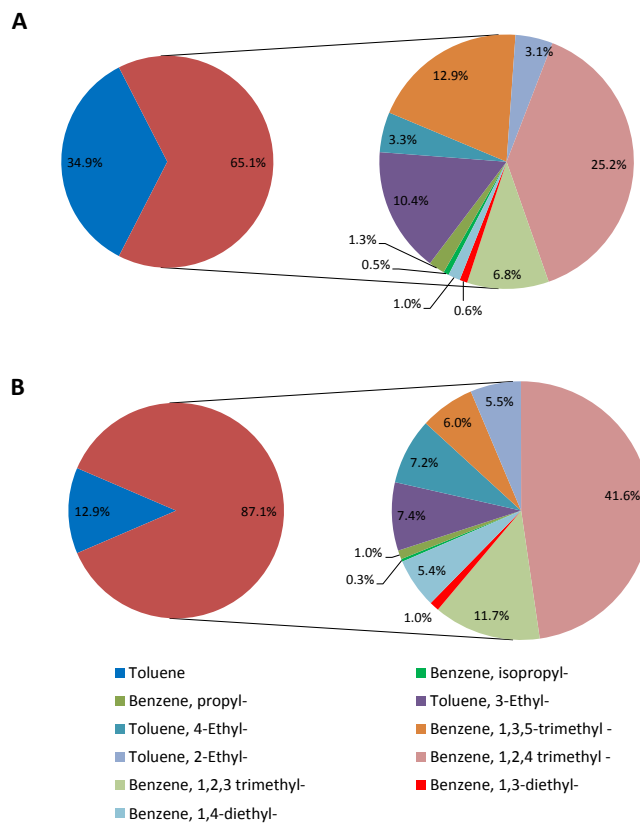


Figure 8. Monocyclic aromatic species contribution to its corresponding $[EQ_{Tol}]$. Red: average $\Sigma[EQ_{Tol}]$. Blue: average toluene mixing ratio. (A) shows contribution for reaction with OH ($[EQ_{Tol}]_{OH}$). (B) shows contribution for reaction with NO_3 ($[J_{Tol}]_{NO_3}$).

sampled containing well-mixed source material with minimal OH losses. Many of the samples collected in this study were taken off the coast of the UK, (the North Sea and the English Channel) providing a well-mixed, integrated assessment of the more highly reactive VOC-to-toluene ratio. This is in contrast to surface measurements which can sometimes be affected by localised sources.

3.3 Effect of additional aromatic VOCs on ambient OH reactivity

The representation of the additional aromatic loading by means of a $[EQ_{Tol}]$ value could potentially be used by atmospheric models as a means of accounting for additional radical reactivity. The OH reactivity (k') is the total pseudo first-order rate coefficient for the loss of OH in the atmosphere and is defined by Eq. (2).

$$k' = \sum_n^{i=1} k_i \cdot [X]_i, \quad (2)$$

where $[X]_i$ and k_i are the concentrations and bimolecular rate coefficients for the i th species reacting with OH. Previous field-based studies with extensive instrumentation (Di Carlo et al., 2004; Sadanaga et al., 2004; Emmerson et al., 2007; Lee et al., 2009; Mao et al., 2009; Sinha et al., 2010; Stone et al., 2012) consistently find that measured OH reactivity is unaccounted for when compared to the directly measured OH sinks, which is often attributed to unmeasured VOCs. The potential additional contribution of the newly resolved aromatic species measured in this study to the OH reactivity measured/calculated for two UK ground-based summertime field campaigns was investigated using campaign-tailored chemical box models incorporating the Master Chemical Mechanism (MCMv3.1), constrained using the comprehensive range of measurements obtained from each campaign. The first Tropospheric ORganic CHEmistry experiment (TORCH 1) took place during the severe Europe-wide August heatwave of summer 2003 at Writtle (51°44'12" N, 0°25'28" E), a rural site approximately 25 miles (40 km) north-east of London (Lee et al., 2006). Observations covered the period of extreme temperatures and high ozone concentrations as well as more typical summertime westerly cyclonic conditions both before and after this event. The modelling work discussed here focuses on the heatwave period (5 to 11 August 2003) only. The TORCH 1 base model simulation runs for this work are similar to those described in Emmerson et al. (2007).

The TORCH 2 study took place in May 2004 at the Weybourne Atmospheric Observatory (WAO), situated on the north Norfolk coast (Lee et al., 2009). During the study, WAO (52°57'23" N, 1°7'40" E) was subjected to similar air masses to those encountered during RONOCO (predominantly from a north-easterly direction). As part of the comprehensive suite of observations carried out during this study,

an OH lifetime instrument was used to measure the temporal decay of artificially produced OH radicals with its ambient sinks in an atmospheric flow tube reactor (Ingham et al., 2009). The OH reactivity measurement was then compared to the reactivity calculated from the individual species measured at the site using Eq. (2). For much of the measurement period there was a difference between the measured and calculated k' , with the average value of $k'_{meas} - k'_{calc} = 1.9 \text{ s}^{-1}$. In addition, the measured species were used as the inputs to a zero-dimensional box model using the full MCM chemistry scheme (i.e. the base case TORCH 2 model discussed in this work). The discrepancy between the measured and calculated k' was reduced to 1.27 s^{-1} , owing to the production of reactive oxygenated intermediates in the model that are not directly measured during the campaign and therefore were not included in the basic calculation. Although the addition of these oxygenated species has reduced the discrepancy between measured and modelled reactivity, there is still a significant degree that remains. To account for this missing reactivity with a surrogate unmeasured species of reactivity similar to *o*-xylene would require a mixing ratio of approximately 4.0 ppbv. Similarly, the missing reactivity could be accounted for by a thousand unidentified species with a mixing ratio of about 10 pptv and a rate constant equal to octane (the highest molecular weight species measured during the study).

The $[EQ_{Tol}]_{OH}$ values derived in this study have been used to investigate the impact of the higher monoaromatic species on OH reactivity during the two TORCH campaigns. The TORCH 1 and 2 models (as described in more detail in Emmerson et al. (2007) and Lee et al. (2009) respectively) were modified using the $\Sigma[EQ_{Tol}]_{OH}$ values obtained during RONOCO to account for the additional aromatic loadings over the original VOC data (the base case). Two model runs were performed for each campaign. The first model run (primary case) was performed using a dummy molecule in the simulation with the same k_{OH} as toluene. This molecule was added into the model at $2 \times [Tol]$ (i.e. from $\Sigma[EQ_{Tol}]_{OH}$ versus $[Tol]$ in Fig. 7). The second model run (secondary case) was performed by simply increasing the toluene mixing ratio by a factor of 3 (i.e. $[Tol] + \Sigma[EQ_{Tol}]_{OH}$). The increased toluene mixing ratio in the secondary case was then allowed to react to form oxidation products, resulting in further compounds that could react with OH. The additional reactivity calculated using the modified models for the two TORCH campaigns are shown in Fig. 9. The red traces show the difference between the primary case and the base case and the blue traces show the difference between the secondary case and the base case. Both the TORCH 1 and TORCH 2 data show a similar increase in predicted k' values over the base case at 0.5–6.0%. The TORCH 1 data, however, show a larger increase in reactivity over the base rate of between 0.1 and 1.0 s^{-1} . This is in contrast to the TORCH 2 data, with a range of between 0.02 and 0.2 s^{-1} .

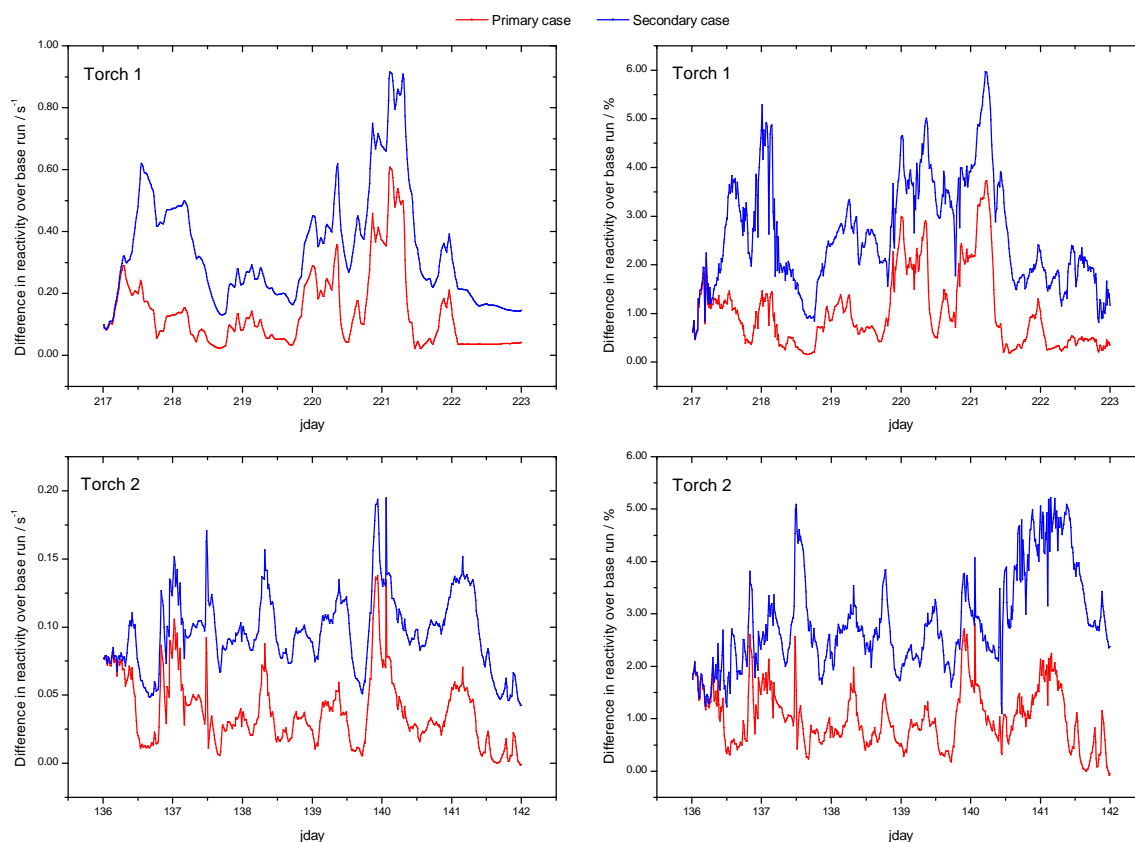


Figure 9. Modified model data for the TORCH 1 and 2 campaigns. Plots show a difference in reactivity over the original model base case whereby VOC aromatic reactivity has been supplemented using the proportionality factor determined in Fig. 6. The red trace shows the difference between the base case and the primary case, which has the additional aromatic content represented by an additional species with the same reactivity as toluene, but after initial reaction it does not yield further oxidation products. The blue trace shows the difference between the base case and the secondary case where the toluene mixing ratio has been increased to account for the additional aromatic reactivity and secondary reactions are included. Jday = Julian day

The difference in absolute reactivity for the secondary case in the TORCH 1 data, although only a small percentage difference, is still a significant value at a maximum of 1 s^{-1} . The simulations presented here serve to show that the addition of only 10 low abundance aromatics to the model can potentially provide an appreciable extra sink for OH. However, the major assumptions are (i) that the MCM toluene photooxidation scheme can be used as a surrogate mechanism to estimate the contribution of the secondary photochemistry of the 10 unmeasured monoaromatics to the additional OH reactivity, and (ii) that the EQ_{Tol} values derived are applicable to those found over the UK/European region.

4 Conclusions

Data collected from a series of UK coastal and free-tropospheric flights during the winter 2011 RONOCO flying campaign have shown that GC × GC-TOFMS is a useful tool for the atmospheric analysis of larger monoaromatic compounds. The technique has excellent resolution

and sensitivity and is reliable with quantified values in good agreement with the established FGAM DC-GC-FID instrument. The added sensitivity and resolution is particularly useful in the detection and quantification of many species that more established methods like GC-FID and PTRMS cannot isolate, particularly at higher molecular weights. From the VOC data measured during RONOCO it was observed that many of the higher molecular weight aromatics exhibited a strong correlation with toluene, indicating similar anthropogenic sources. Assuming this relationship is consistent, the use of the proportionality factors (EQ_{Tol}) obtained here can be used to predict the mixing ratios of these additional aromatic species without needing to measure them directly. Adding 10 previously unaccounted for monoaromatic compounds to model simulations of both polluted and rural chemistry increased the total simulated OH reactivity by up to 6 %, bringing the modelled OH reactivity more into line with the measurements. The proportionality factors were determined using VOC measurements taken under a range of different air masses, from localised pollution to aged regional

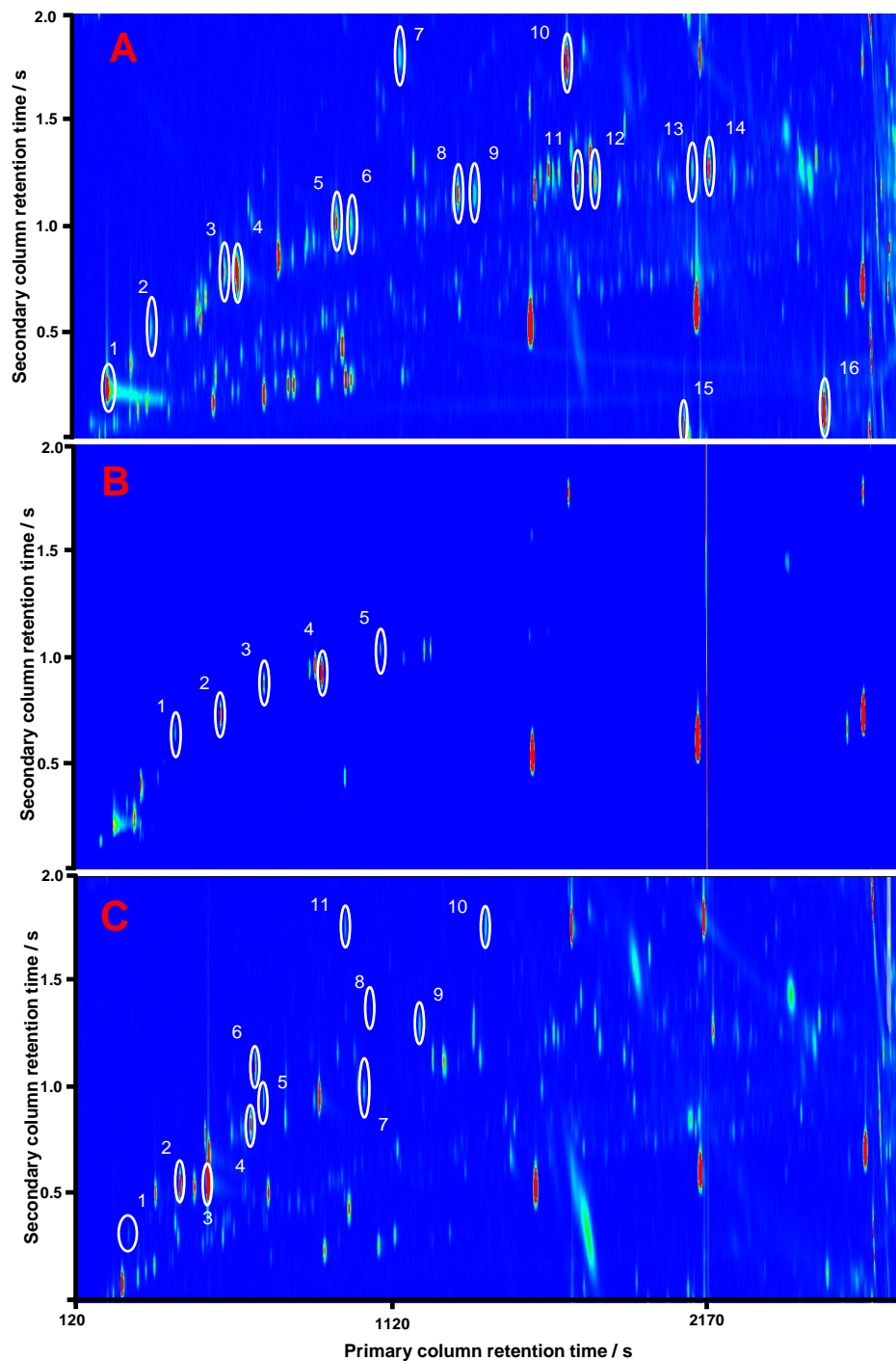


Figure 10. Typical chromatogram from a sample taken during RONOCO (flight B570 canister 34). **(A)** EIC of m/z 58 + 95 + 112 + 120 + 128, highlighting the presence of oxygenated species. Labelled peaks are identified as follows: (1) acetone, (2) 2-butanone, (3) 2-pentanone, (4) pentanal, (5) 2-hexanone, (6) hexanal, (7) furfural, (8) 2-heptanone, (9) heptanal, (10) phenol, (11) 2-octanone, (12) octanal, (13) 2-nonanone, (14) nonanal, (15) acetophenone and (16) naphthalene. **(B)** EIC m/z 46, highlighting the presence of alkyl nitrate species. Labelled peaks are identified as follows: (1) ethyl nitrate, (2) isopropyl nitrate, (3) propyl nitrate, (4) *sec*-butyl nitrate and (5) butyl nitrate. **(C)** EIC m/z 63 + 83 + 86 + 93 + 112 + 117 + 166 + 170 + 172 + 174, highlighting the presence of halocarbon species. Labelled peaks are identified as follows: (1) dichloromethane, (2) chloroform, (3) carbon tetrachloride, (4) 1,2-dichloropropane, (5) bromodichloromethane, (6) dibromomethane, (7) tetrachloroethylene, (8) dibromochloromethane, (9) chlorobenzene, (10) tribromomethane and (11) 2-iodopropane.

background, and so should be typical for the UK. However, more work is needed to study whether these scaling factors are consistent at other locations.

TD-GC × GC-TOFMS has the ability to detect and resolve many other functionalities of atmospherically relevant species such as higher molecular weight multifunctional volatile oxygenates, halocarbons and alkyl nitrates shown in Fig. 10. Quantification of many of the species detected within this study was not possible owing to a lack of appropriate standards and unknown stability within the WAS canisters. Their impact is also uncertain since in many cases kinetic data are not available. In the future it would be possible to develop an atmospheric sampling method that has the potential to target all these species, within a single analysis, if standards for these species were available.

The Supplement related to this article is available online at doi:10.5194/acp-14-6677-2014-supplement.

Acknowledgements. R. T. Lidster would like to thank the Natural Environment Research Council (NERC) and RONOCO for studentship funding (NE/F004354/1).

Airborne data was obtained using the BAe-146-301 Atmospheric Research Aircraft [ARA] flown by Directflight Ltd and managed by the Facility for Airborne Atmospheric Measurements [FAAM], which is a joint entity of NERC and the Met Office.

Edited by: J. Roberts

References

- Apel, E. C., Brauers, T., Koppmann, R., Bandowe, B., Boßmeyer, J., Holzke, C., Tillmann, R., Wahner, A., Wegener, R., Brunner, A., Jocher, M., Ruuskanen, T., Spirig, C., Steigner, D., Steinbrecher, R., Gomez Alvarez, E., Müller, K., Burrows, J. P., Schade, G., Solomon, S. J., Ladstätter-Weissenmayer, A., Simmonds, P., Young, D., Hopkins, J. R., Lewis, A. C., Legreid, G., Reimann, S., Hansel, A., Wisthaler, A., Blake, R. S., Ellis, A. M., Monks, P. S., and Wyche, K. P.: Intercomparison of oxygenated volatile organic compound measurements at the SAPHIR atmosphere simulation chamber, *J. Geophys. Res. Atmos.*, 113, D20307, doi:10.1029/2008JD009865, 2008.
- Atkinson, R.: Atmospheric chemistry of VOCs and NO_x, *Atmos. Environ.*, 34, 2063–2101, 2000.
- Atkinson, R. and Arey, J.: Gas-phase tropospheric chemistry of biogenic volatile organic compounds: a review, *Atmos. Environ.*, 37, 197–219, 2003.
- Bartenbach, S., Williams, J., Plass-Dülmer, C., Berresheim, H., and Lelieveld, J.: In-situ measurement of reactive hydrocarbons at Hohenpeissenberg with comprehensive two-dimensional gas chromatography (GC × GC-FID): use in estimating HO and NO₃, *Atmos. Chem. Phys.*, 7, 1–14, doi:10.5194/acp-7-1-2007, 2007.
- Brown, H. C. and Okamoto, Y.: Electrophilic Substituent Constants, *J. Am. Chem. Soc.*, 80, 4979–4987, doi:10.1021/ja01551a055, 1958.
- Calvert, J. G., Atkinson, R., Becker, K. H., Kamens, R. M., Seinfeld, J. H., Wallington, T. J., and Yarwood, G.: *The Mechanisms of Atmospheric Oxidation of Aromatic Hydrocarbons*, Oxford University Press, 2002.
- Chameides, W. L., Fehsenfeld, F., Rodgers, M. O., Cardelino, C., Martinez, J., Parrish, D., Lonneman, W., Lawson, D. R., Rasmussen, R. A., Zimmerman, P., Greenberg, J., Middleton, P., and Wang, T.: Ozone Precursor Relationships in the Ambient Atmosphere, *J. Geophys. Res.*, 97, 6037–6055, 1992.
- Di Carlo, P., Brune, W. H., Martinez, M., Harder, H., Leshner, R., Ren, X., Thornberry, T., Carroll, M. A., Young, V., Shepson, P. B., Riemer, D., Apel, E., and Campbell, C.: Missing OH Reactivity in a Forest: Evidence for Unknown Reactive Biogenic VOCs, *Science*, 304, 722–725, doi:10.1126/science.1094392, 2004.
- Emmerson, K. M., Carslaw, N., Carslaw, D. C., Lee, J. D., McFiggans, G., Bloss, W. J., Gravestock, T., Heard, D. E., Hopkins, J., Ingham, T., Pilling, M. J., Smith, S. C., Jacob, M., and Monks, P. S.: Free radical modelling studies during the UK TORCH Campaign in Summer 2003, *Atmos. Chem. Phys.*, 7, 167–181, doi:10.5194/acp-7-167-2007, 2007.
- Goldstein, A. H. and Galbally, I. E.: Known and Unexplored Organic Constituents in the Earth's Atmosphere, *Environ. Sci. Technol.*, 41, 1514–1521, 2007.
- Hamilton, J. F. and Lewis, A. C.: Monoaromatic complexity in urban air and gasoline assessed using comprehensive GC and fast GC-TOF/MS, *Atmos. Environ.*, 37, 589–602, 2003.
- Heard, D. E. and Pilling, M. J.: Measurement of OH and HO₂ in the troposphere, *Chem. Rev.*, 103, 5163–5198, 2003.
- Hopkins, J. R., Boddy, R. K., Hamilton, J. F., Lee, J. D., Lewis, A. C., Purvis, R. M., and Watson, N. J.: An observational case study of ozone and precursors inflow to South East England during an anticyclone, *J. Environ. Monitor.*, 8, 1195–1202, 2006.
- Hopkins, J. R., Jones, C. E., and Lewis, A. C.: A dual channel gas chromatograph for atmospheric analysis of volatile organic compounds including oxygenated and monoterpene compounds, *J. Environ. Monitor.*, 13, 2268–2276, 2011.
- Ingham, T., Goddard, A., Whalley, L. K., Furneaux, K. L., Edwards, P. M., Seal, C. P., Self, D. E., Johnson, G. P., Read, K. A., Lee, J. D., and Heard, D. E.: A flow-tube based laser-induced fluorescence instrument to measure OH reactivity in the troposphere, *Atmos. Meas. Tech.*, 2, 465–477, doi:10.5194/amt-2-465-2009, 2009.
- Jenkin, M. E., Saunders, S. M., Wagner, V., and Pilling, M. J.: Protocol for the development of the Master Chemical Mechanism, MCM v3 (Part B): tropospheric degradation of aromatic volatile organic compounds, *Atmos. Chem. Phys.*, 3, 181–193, doi:10.5194/acp-3-181-2003, 2003.
- Kovacs, T. and Brune, W.: Total OH Loss Rate Measurement, *J. Atmos. Chem.*, 39, 105–122, doi:10.1023/A:1010614113786, 2001.
- Kwok, E. S. C. and Atkinson, R.: Estimation of hydroxyl radical reaction-rate constants for gas-phase organic-compounds using a structure-reactivity relationship – an update, *Atmos. Environ.*, 29, 1685–1695, 1995.

- Lee, J., Young, J., Read, K., Hamilton, J., Hopkins, J., Lewis, A., Bandy, B., Davey, J., Edwards, P., Ingham, T., Self, D., Smith, S., Pilling, M., and Heard, D.: Measurement and calculation of OH reactivity at a United Kingdom coastal site, *J. Atmos. Chem.*, 64, 53–76, 2009.
- Lee, J. D., Lewis, A. C., Monks, P. S., Jacob, M., Hamilton, J. F., Hopkins, J. R., Watson, N. M., Saxton, J. E., Ennis, C., Carpenter, L. J., Carslaw, N., Fleming, Z., Bandy, B. J., Oram, D. E., Penkett, S. A., Slemr, J., Norton, E., Rickard, A. R., K Whalley, L., Heard, D. E., Bloss, W. J., Gravestock, T., Smith, S. C., Stanton, J., Pilling, M. J., and Jenkin, M. E.: Ozone photochemistry and elevated isoprene during the UK heatwave of August 2003, *Atmos. Environ.*, 40, 7598–7613, 2006.
- Lewis, A. C., Carslaw, N., Marriott, P. J., Kinghorn, R. M., Morrison, P., Lee, A. L., Bartle, K. D., and Pilling, M. J.: A larger pool of ozone-forming carbon compounds in urban atmospheres, *Nature*, 405, 778–781, 2000.
- Lewis, A. C., Evans, M. J., Hopkins, J. R., Punjabi, S., Read, K. A., Purvis, R. M., Andrews, S. J., Moller, S. J., Carpenter, L. J., Lee, J. D., Rickard, A. R., Palmer, P. I., and Parrington, M.: The influence of biomass burning on the global distribution of selected non-methane organic compounds, *Atmos. Chem. Phys.*, 13, 851–867, doi:10.5194/acp-13-851-2013, 2013.
- Logan, J. A., Prather, M. J., Wofsy, S. C., and McElroy, M. B.: Tropospheric Chemistry: A Global Perspective, *J. Geophys. Res.*, 86, 7210–7254, 1981.
- Mao, J., Ren, X., Brune, W. H., Olson, J. R., Crawford, J. H., Fried, A., Huey, L. G., Cohen, R. C., Heikes, B., Singh, H. B., Blake, D. R., Sachse, G. W., Diskin, G. S., Hall, S. R., and Shetter, R. E.: Airborne measurement of OH reactivity during INTEX-B, *Atmos. Chem. Phys.*, 9, 163–173, doi:10.5194/acp-9-163-2009, 2009.
- Nölscher, A. C., Sinha, V., Bockisch, S., Klüpfel, T., and Williams, J.: Total OH reactivity measurements using a new fast Gas Chromatographic Photo-Ionization Detector (GC-PID), *Atmos. Meas. Tech.*, 5, 2981–2992, doi:10.5194/amt-5-2981-2012, 2012.
- Phillips, J. and Liu, Z.: Comprehensive Two-dimensional Gas Chromatography using an On-Column Thermal Modulator Interface, *J. Chromatogr. Sci.*, 28, 227–231, 1991.
- RONOCO: FAAM, <http://www.faam.ac.uk/index.php/campaigns/current-campaigns/85-ronoco>, 2009–2011.
- Sadanaga, Y., Yoshino, A., Watanabe, K., Yoshioka, A., Wakazono, Y., Kanaya, Y., and Kajii, Y.: Development of a measurement system of OH reactivity in the atmosphere by using a laser-induced pump and probe technique, *Rev. Sci. Instr.*, 75, 2648–2655, doi:10.1063/1.1775311, 2004.
- Saxton, J. E., Lewis, A. C., Kettlewell, J. H., Ozel, M. Z., Gogus, F., Boni, Y., Korogone, S. O. U., and Serca, D.: Isoprene and monoterpene measurements in a secondary forest in northern Benin, *Atmos. Chem. Phys.*, 7, 4095–4106, doi:10.5194/acp-7-4095-2007, 2007.
- Sinha, V., Williams, J., Crowley, J. N., and Lelieveld, J.: The comparative reactivity method - a new tool to measure total OH reactivity in ambient air, *Atmos. Chem. Phys.*, 8, 2213–2227, doi:10.5194/acp-8-2213-2008, 2008.
- Sinha, V., Williams, J., Lelieveld, J., Ruuskanen, T., Kajos, M., Patokoski, J., Hellen, H., Hakola, H., Mogensen, D., Boy, M., Rinne, J., and Kulmala, M.: OH Reactivity Measurements within a Boreal Forest: Evidence for Unknown Reactive Emissions, *Environ. Sci. Technol.*, 44, 6614–6620, doi:10.1021/es101780b, 2010.
- Stone, D., Evans, M. J., Commane, R., Ingham, T., Floquet, C. F. A., McQuaid, J. B., Brookes, D. M., Monks, P. S., Purvis, R., Hamilton, J. F., Hopkins, J., Lee, J., Lewis, A. C., Stewart, D., Murphy, J. G., Mills, G., Oram, D., Reeves, C. E., and Heard, D. E.: HO_x observations over West Africa during AMMA: impact of isoprene and NO_x, *Atmos. Chem. Phys.*, 10, 9415–9429, doi:10.5194/acp-10-9415-2010, 2010.
- Stone, D., Whalley, L. K., and Heard, D. E.: Tropospheric OH and HO₂ radicals: field measurements and model comparisons, *Chem. Soc. Rev.*, 41, 6348–6404, doi:10.1039/C2CS35140D, 2012.
- Xu, X., Stee, L. L. P., Williams, J., Beens, J., Adahchour, M., Vreuls, R. J. J., Brinkman, U. A., and Lelieveld, J.: Comprehensive two-dimensional gas chromatography (GC × GC) measurements of volatile organic compounds in the atmosphere, *Atmos. Chem. Phys.*, 3, 665–682, doi:10.5194/acp-3-665-2003, 2003a.
- Xu, X., Williams, C., Plass-Dülmer, H., Berresheim, H., Salisbury, G., Lange, L., and Lelieveld, J.: GC × GC measurements of C₇–C₁₁ aromatic and n-alkane hydrocarbons on Crete, in air from Eastern Europe during the MINOS campaign, *Atmos. Chem. Phys.*, 3, 1461–1475, doi:10.5194/acp-3-1461-2003, 2003b.